Shaping Laguerre–Gaussian laser modes with binary gratings using a digital micromirror device

Vitaly Lerner, David Shwa, Yehonathan Drori, and Nadav Katz*

Racah Institute of Physics, Hebrew University of Jerusalem, Jerusalem 91904, Israel
**Corresponding author: katzn@phys.huji.ac.il*

Received September 19, 2012; revised October 9, 2012; accepted October 9, 2012;
posted October 17, 2012 (Doc. ID 176469); published November 16, 2012

Laguerre–Gaussian (LG) beams are used in many research fields, including microscopy, laser cavity modes, and optical tweezing. We developed a holographic method to generate pure LG modes (amplitude and phase) with a binary amplitude-only digital micromirror device (DMD) as an alternative to the commonly used phase-only spatial light modulator. The advantages of such a DMD include very high frame rates, low cost, and high damage thresholds. We have shown that the propagating shaped beams are self-similar and their phase fronts are of helical shape as demanded. We estimate the purity of the resultant beams to be above 94%. © 2012 Optical Society of America

OCIS codes: 030.4070, 090.1995, 120.4820, 140.3300.

Laguerre–Gaussian (LG) laser beam modes are solutions of the scalar Helmoltz equation under the paraxial approximation [1]. Since LG beam modes carry an angular momentum [2], they have been intensively investigated and are widely used in many research fields, including optical tweezing and atom guiding [3,4], second-harmonic generation [5], quantum information, and communication [6].

Much of the work done on beam shaping has been carried out recently with phase-only spatial light modulators (SLMs) [7–9]. An alternative to this method is an amplitude control, using a digital micromirror device (DMD). The most significant advantage of the DMD over liquid crystal on silicon (LCoS) SLM is frame rate [10,11]. While LG modes have been generated using static amplitude holograms [12], here we focus on programmable patterns. LG amplitude [13] and helical phase [14] have been generated separately using a DMD, while we focus on pure LG modes (both amplitude and phase).

Mathematically, LG modes are described in cylindrical coordinates, where we rescale r, z by the beam width w_0 and corresponding Rayleigh range $z_0 = \pi w_0^2/\lambda$: $\rho = r/w_0$; $\zeta = z/z_0$. The width of all such Gaussian beams, at distance ζ from the waist is $R(\zeta) = \sqrt{1 + 4\zeta^2}$. We can write the electric field of a LG mode [1] using generalized Laguerre polynomials $L_p^l(x)$, separated to amplitude and phase, omitting the global normalization constants and the global phase due to the propagation distance:

$$|u_p^l(\rho, \varphi, \zeta)| = \left(\frac{2\rho^2}{R^2(\zeta)}\right)^{|l|} L_p^{|l|}\left(\frac{2\rho^2}{R^2(\zeta)}\right) \exp\left(-\frac{\rho^2}{R^2(\zeta)}\right) \quad (1)$$

and

$$\Phi\{u_p^l(\rho, \varphi, \zeta)\} = l\varphi + \frac{\rho^2}{R^2(\zeta)}\zeta. \quad (2)$$

Although shaping a phase front [Eq. (2)] is a relatively simple procedure when using a phase-only SLM such as LCoS, shaping an amplitude pattern is a matter of considerable algorithmic work [8]. In our case, the situation is the opposite: We used an amplitude-only SLM. It is very easy to load a pattern on the DMD and to observe the same pattern at the imaging plane, but a phase front cannot be created directly. A convenient technique [12,14–16] to create light vortices of type $\Phi_l(\varphi) = l\varphi$ is to use a fork-like pattern as shown in Fig. 1(c). The pattern is a holographic interference of an LG beam with a unitary planar beam. Assuming that the angle between the beams is α and the LG beam is at its waist ($\zeta = 0$, $R(\zeta = 0) = 1$), the phase front becomes

$$\Phi_l(\rho, \varphi) = l\varphi + \frac{2\pi}{\lambda}\rho \cos\varphi \sin\alpha. \quad (3)$$

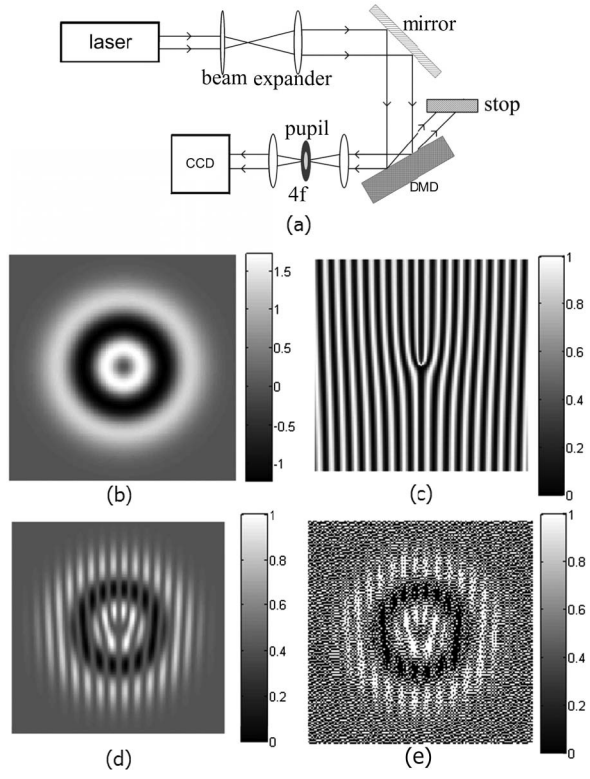

Fig. 1. (a) Schematic of the experimental setup; (b)–(e) shaping amplitude and phase of LG_2^2 mode (all patterns are 240 × 240 px, corresponding to 1.8 × 1.8 mm); (b) ideal amplitude; (c) fork-like hologram for $l = 2$; (d) normalized multiplication of (b) by (c); and (e) dithered pattern loaded on the DMD. Note that the background corresponds to half filling to allow for negative amplitude of alternate rings in the LG pattern.

The diffraction grating we used for creating such a front is

$$I_l(\rho,\varphi) = \cos(\Phi_l(\rho,\varphi)). \quad (4)$$

We used a DMD mounted in a Texas Instruments Pico DLP projector v.2 in a manner similar to that of [17]. We worked at a video rate since our goal was a proof-of-concept. Other control platforms, with higher [11] bandwidth, are available. The DMD consists of 480×320 micromirrors, each 7.6 microns $\times$ 7.6 microns in size. Each mirror corresponds to a certain pixel and is held in either of two angular positions: $+12°$ (on, or "white" state) and $-12°$ (off, or "black") state [18]. The DMD served as a programmable spatial filter since the light reflected from and diffracted by the mirrors corresponding to the black pixels is filtered out (Fig. 1).

The maximal efficiency of a grey amplitude hologram is known to be $1/6 = 6.25\%$, while for binary amplitude it can reach $1/\pi^2 \sim 10.1\%$ [19,20]. Due to the complex three-dimensional structure of the DMD surface, the pattern effectively consists of two gratings: the micromirror's grating-like structure and the information grating. When all pixels are on at a particular angle, we concentrated more than 88% [18,21] of the diffracted light into a single order. We measured an additional loss of about 40% of the total power of the incident beam. After applying the information grating between 1% and 5% of the incident beam intensity was concentrated in an output beam.

To obtain a desired pattern at the imaging plane, the pupil transferred the first order beam and filtered the other diffraction beams [Fig. 1(a)]. In our experiments, 40 cm away from the DMD the beams were well separated. However, to reproduce the near field, we used the imaging system.

We created two optical vortices (i.e., diffractions of $\pm$1st orders) by applying a fork-like pattern [Eq. (4), Fig. 1(c)]. A similar method is described in [14], where slow grey-scale pixel modulation was used. However, many applications require stable vortex patterns. Therefore, we avoid modulating pixels in time and resort to pixel dithering [22]. The dithering leads to effective grey scale amplitude control.

The fork-like patterns are used to create vortices with no direct control of the amplitude. Ring-like amplitude has been achieved in previous works [12] by $\pi/2$-shifts at the zeros of LG radial component of amplitude distribution. We apply a different method, achieving significantly higher purity of the LG modes. We separated the beam shape into its amplitude and phase components [Eqs. (1) and (3)]. We then multiplied the fork-like pattern by the amplitude distribution and dithered the resultant pattern (Fig. 1).

Previous works [8,12] have shown that the purity of the LG modes was significantly affected by the ratio of the normalization radius of the hologram and the input Gaussian beam. Even at the optimal value of this ratio, the purity of the LG modes with $p > 1$ was low when an amplitude-only hologram was applied to Gaussian beam [12]. We optimize the purity of the output beams by changing the applied pattern:

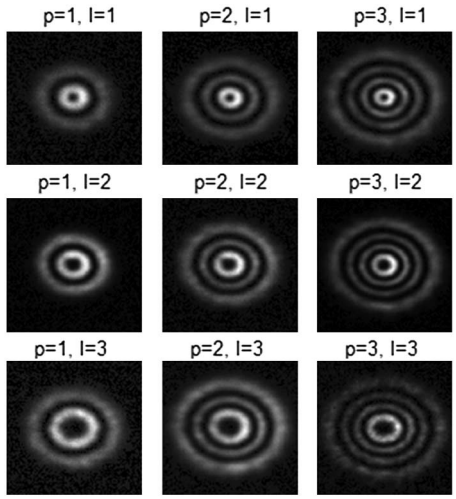

Fig. 2. Intensities in the far field. The radius of the outer ring of the LG_3^3 beam is 700 μm.

$$\left|u_p^{l\,\mathrm{corr}}(r,\varphi,z=0)\right| = \left(\frac{2r^2}{w^2}\right)^l L_p^l\left(\frac{2r^2}{w^2}\right)\exp\left(-p_0\cdot\frac{r^2}{w^2}\right), \quad (5)$$

where $p_0 = w^2/w_{\mathrm{env}}^2 = 1 - w^2/w_i^2$ is a correction parameter, w_i is the width of the incident Gaussian beam, w_{env} is the corrected width of the Gaussian envelope of the pattern and w is the desired width of the shaped LG mode. The correction parameter can be calculated from measurements and substituted back to Eq. (5), but it should be fine-tuned empirically.

We measured a minimal radius where there is no distortion of the resultant mode and a good off/on ratio to be 12 pixels (corresponding to about 90 μm).

The results obtained at the imaging plane and in the near field show no significant difference from the far field, proving that the obtained modes are true LG modes [Eq. (1)]. Figure 2 shows the results in far field [23]. To ensure that the far field is measured, and to focus the beam on the camera, we placed a convex lens ($f = 20$ cm) exactly 20 cm from the camera and 50 cm from the DMD. The Rayleigh range of the resultant beam was 12 cm. To study intensity profiles, we plotted cross-sections along with the ideal mode's intensity profiles (Fig. 3). To confirm the helical phase front, the resultant beams are interfered with an off-axis Gaussian beam. Figure 4 shows the center of the resultant pattern, and its fork-like shape confirms [15] that the beam has a helical phase front in the far field.

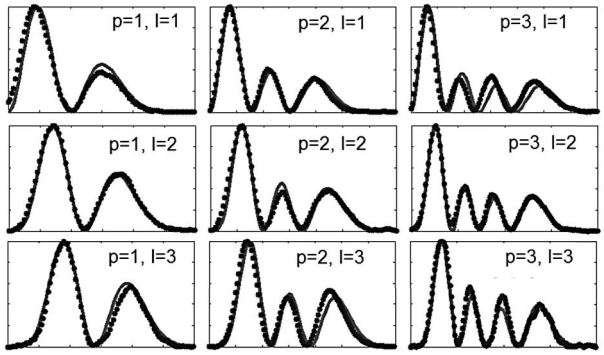

Fig. 3. Radial profiles of intensity obtained from cross sections of Fig. 2 (dotted) versus ideal LG intensity profiles (solid).

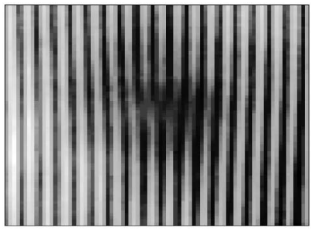

Fig. 4. Interference of an LG_0^1 beam with an off-axis Gaussian beam in far field (Physical height: 100 μm).

The experimental results fit almost perfectly the ideal intensity profiles. The off:on ratio (intensity at the origin divided by maximal intensity) varies between 1∶100 and 1∶1000.

To give a quantitative measure of the beams' quality, we calculated mode purity in a manner similar to [9]. Since we only measured intensity and not amplitude or phase, we used a simulation of far-field Fraunhoffer diffraction to estimate the mode purity. As an input, we used the same pattern loaded on the DMD multiplied by a Gaussian beam. Both simulation field $u^l_{p,\mathrm{sim}}(r,\varphi)$ and ideal one $u^l_{p,\mathrm{id}}(r,\varphi)$ are normalized. We define purity as

$$P^l_p = \left| \iint u^l_{p,\mathrm{sim}} * \cdot u^l_{p,\mathrm{id}} \cdot r \mathrm{d}r\mathrm{d}\varphi \right|^2. \tag{6}$$

The results for different modes vary from 95% (P_3^3) to 97% (P_2^1).

A simpler direct correlation overlap of the experimental results (intensities) with the ideal intensities (Fig. 3) yields slightly lower results (between 94% and 96%). This indicates that, experimentally, we are very close to the optimal reachable result using this method.

In summary, we used a DMD as an amplitude-only SLM and demonstrated the shaping of LG modes. We achieved high purity, above 94%, of the modes, and we have shown that such purity is nearly optimal when our method is used. Further improvements may include employing a higher-resolution DMD, and a fine adjustment of patterns in closed loop control.

We thank Nir Davidson and Hagai Eisenberg for helpful suggestions and discussion. This research was supported by ISF grant 1248/10.

References and Notes

1. M. Padgett and L. Allen, Opt. Commun. **121**, 36 (1995).
2. L. Allen, M. Beijersbergen, R. Spreeuw, and J. Woerdman, Phys. Rev. A **45**, 8185 (1992).
3. A. T. O'Neill and M. J. Padgett, Opt. Commun. **193**, 45 (2001).
4. J. Arlt, T. Hitomi, and K. Dholakia, Appl. Phys. B **71**, 549 (2000).
5. D. Petrov, Phys. Rev. A **82**, 035801 (2010).
6. J. Torres, Y. Deyanova, L. Torner, and G. Molina-Terriza, Phys. Rev. A **67**, 052313 (2003).
7. L. Hu, L. Xuan, Y. Liu, Z. Cao, D. Li, and Q. Mu, Opt. Express **12**, 6403 (2004).
8. N. Matsumoto, T. Ando, T. Inoue, Y. Ohtake, N. Fukuchi, and T. Hara, J. Opt. Soc. Am. A **25**, 1642 (2008).
9. S. A. Kennedy, M. J. Szabo, H. Teslow, J. Z. Porterfield, and E. R. I. Abraham, Phys. Rev. A **66**, 043801 (2002).
10. J. Otona, M. S. Millana, P. Ambs, and E. Perez-Cabrea, Proc. SPIE **7000**, 70001V (2008).
11. F. P. Martial and N. A. Hartell, PLoS ONE **7**, e43942 (2012).
12. J. Arlt, K. Dholakia, L. Allen, and M. J. Padgett, J. Mod. Opt. **45**, 1231 (1998).
13. J. Liyang, "High-precision laser beam shaping and image projection," Ph.D. thesis (University of Texas, 2012).
14. Y. X. Ren, M. Li, K. Huang, J. G. Wu, H. F. Gao, Z. Q. Wang, and Y. M. Li, Appl. Opt. **49**, 1838 (2010).
15. G. Molina-Terriza and J. Torres, Nat. Phys. **3**, 305 (2007).
16. A. Bekshaev and O. Orlinska, Opt. Commun. **283**, 1244 (2010).
17. F. Havermeyer, L. Ho, and C. Moser, Opt. Express **19**, 14642 (2011).
18. L. A. Yoder, W. M. Duncan, E. M. Koontz, J. So, T. A. Bartlett, B. L. Lee, B. D. Sawyers, D. Powell, and P. Rancuret, Proc. SPIE **4457**, 54 (2001).
19. B. R. Brown and A. W. Lohmann, IBM J. Res. Dev. **13**, 160 (1969).
20. A. Lohmann and D. P. Paris, Appl. Opt. **6**, 1739 (1967).
21. D. Dudley, W. M. Duncan, and J. Slaughter, Proc. SPIE **4985**, 14 (2003).
22. R. W. Floyd and L. Steinberg, in *International Symposium Digest of Technical Papers*, *Society for Information Display* (Academic, 1975), p. 36.
23. The barely observable elipticity is due to small imperfections in our tilt angle adjustments, and input Gaussian beam. However, no splitting in $l = 2$ and higher modes was observed, indicating that this imperfection is negligible.